Electronic Supplementary Material (ESI) for Polymer Chemistry.

Supporting Information

Clarification of the effects of topological isomer on mechanical strength of comb polyurethane

Daisuke Aoki,[1] Hiroharu Ajiro[1]

[1]Graduate School of Materials Science, Nara Institute of Science and Technology, 8916-5 Takayama-cho, Nara 630-0192, Japan.

1. Materials.

Scheme S1. Synthesis of diol-*g*-OEG_m and PU-*g*-OEG_m

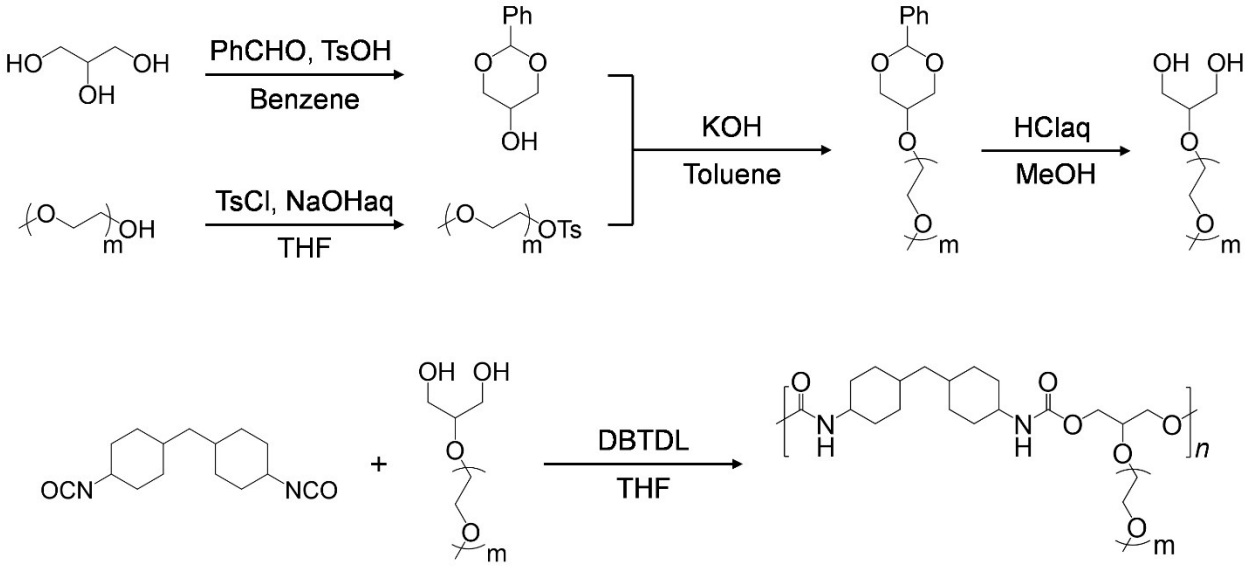

1.1 Synthesis of 2-phenyl-1,3-dioxan-5-ol

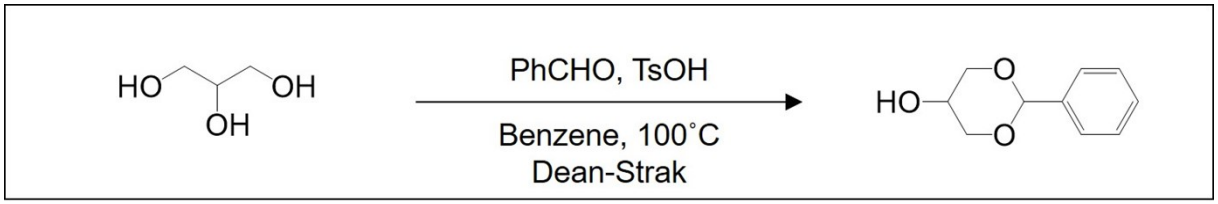

The acetalization of glycerol with benzaldehyde was achieved according to the literature.[1] Glycerol (100 g, 1.1 mol), benzaldehyde (120 g, 1.1 mol), *p*-toluenesulfonic acid monohydrate (2 g, 0.01 mol) were dissolved in 300 mL of benzene and refluxed with a Dean-Stark at 100˚C for 16 h. Then, the reaction mixture was recrystallized in 1600 mL of hexane/toluene (1/1, v/v) at -25˚C. This recrystallization step was repeated at least 3 times until it changed to needle-like crystals. Finally, the needle-like crystals were washed with hexane to obtain the product (64.8g, 360 mmol, yield 36%).

^{1}H NMR (400 MHz, $CDCl_3$): δ3.07 (d, J = 10.0 Hz, 1H, OH), 3.61 (brd, J = 10.0 Hz, 1H), 4.09 (dd, J = 12.0 and 1.5 Hz, 2H), 4.17 (dd, J = 12.0 and 1.5 Hz, 2H), 5.54 (s, 1H), 7.36 (m, 3H), 7.49 (m, 2H).
HRMS (CI) calcd for $C_{10}H_{13}O_3$ [M + H] 181.0865 found 181.08669.

1.2 Synthesis of 5-(2-(2-(2-methoxyethoxy)ethoxy)ethoxy)-2-phenyl-1,3-dioxane

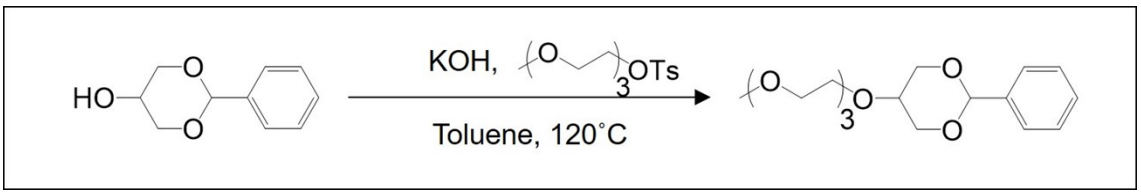

2-phenyl-1,3-dioxan-5-ol (10 g, 56 mmol) and potassium hydroxide (5.6 g, 100 mmol) were refluxed in 200 mL of toluene at 120˚C for 3h with Dean-Stark apparatus to remove water and activated the alcohol. Next, after cooling to room temperature, 2-(2-(2-methoxyethoxy)ethoxy)ethyl 4-methylbenzenesulfonate (19 g, 60 mmol) was introduced with stirring at 80˚C overnight. The reaction mixture was extracted by H_2O and CH_2Cl_2 to collect the organic layer. Then, the crude was purified by silica gel chromatography using hexane/ethyl acetate (1/1, v/v) to obtain (9.1 g, 28 mmol, yield 50%).

^{1}H NMR ($CDCl_3$, 400 MHz) δ:7.50 (m, 2H), 7.38—7.30 (m, 3H), 3.56 (m, 2H), 5.55 (s, 1H), 4.36 (d, 2H), 4.05 (d, 2H), 3.79—3.62 (m, 10H), 3.56—3.52 (m, 2H), 3.42 (q, 1H), 3.38 (s, 3H).
FT-IR(cm^{-1}): 2866, 1450, 1091.
HRMS (CI) calcd for $C_{17}H_{27}O_6$ 327.1808 [M + H] found 327.1802.

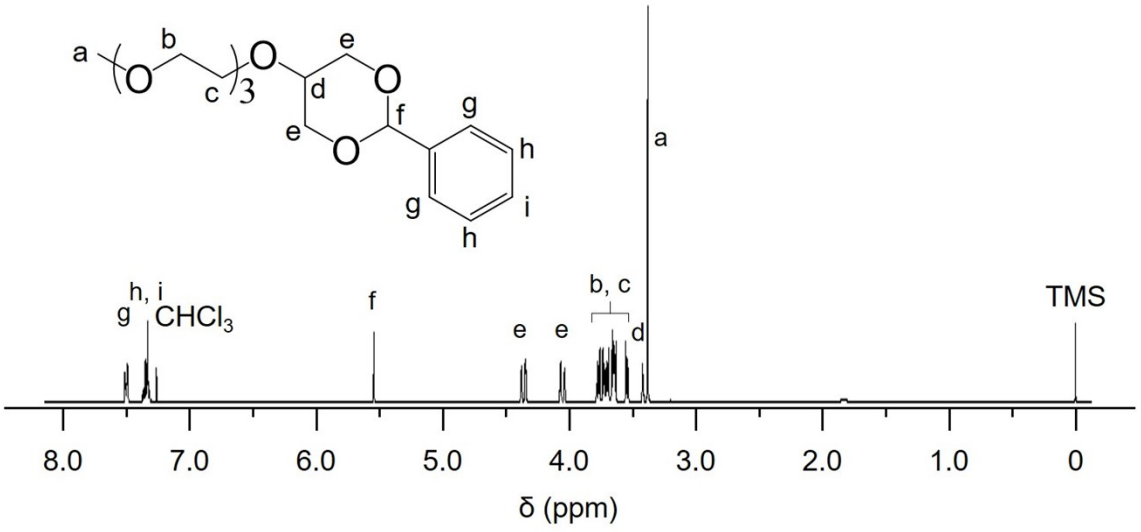

Figure S1. ^{1}H NMR spectrum for 5-(2-(2-(2-methoxyethoxy)ethoxy)ethoxy)-2-phenyl-1,3-dioxane.

1.3 Synthesis of 5-(2-(2-methoxyethoxy)ethoxy)-2-phenyl-1,3-dioxane

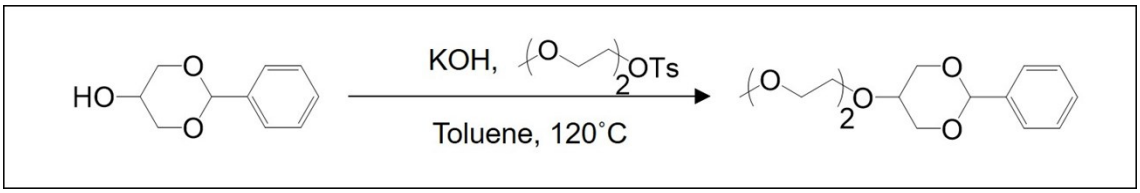

5-(2-(2-methoxyethoxy)ethoxy)-2-phenyl-1,3-dioxane was synthesized in the same procedure as 5-(2-(2-(2-methoxyethoxy)ethoxy)ethoxy)-2-phenyl-1,3-dioxane, except that 2-(2-(2-methoxyethoxy)ethoxy)ethyl 4-methylbenzenesulfonate (16.5 g, 60 mmol) was used instead of 2-(2-methoxyethoxy)ethyl 4-methylbenzenesulfonate (19 g, 60 mmol). The reaction mixture was extracted by H_2O and CH_2Cl_2 to collect the organic layer. Then, the crude was purified by silica gel chromatography using hexane/ethyl acetate (1/1, v/v) to obtain (8.1 g, 27 mmol, yield 48%).

^{1}H NMR ($CDCl_3$, 400 MHz) δ:7.50 (m, 2H), 7.38—7.30 (m, 3H), 3.56 (m, 2H), 5.55 (s, 1H), 4.36 (d, 2H), 4.05 (d, 2H), 3.79—3.62 (m, 10H), 3.56—3.52 (m, 2H), 3.42 (q, 1H), 3.38 (s, 3H).
FT-IR(cm^{-1}): 2870, 1450, 1095.
HRMS (ESI) calcd for $C_{15}H_{22}Na_1O_5$ 305.13649 [M + Na] found 305.13597.

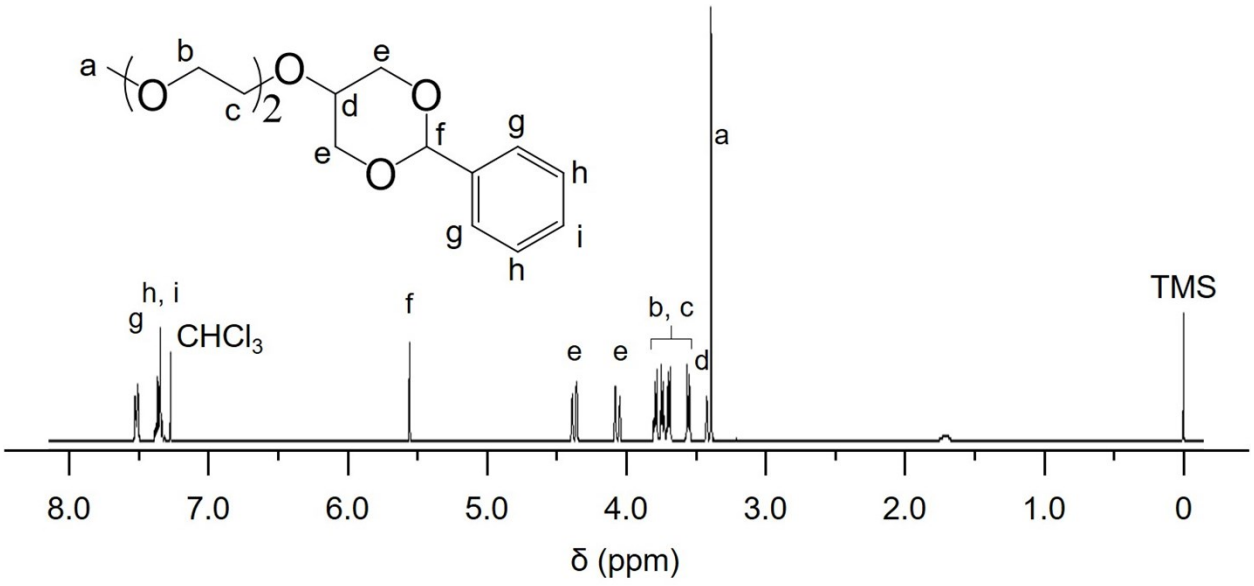

Figure S2. ^{1}H NMR spectrum for 5-(2-(2-methoxyethoxy)ethoxy)-2-phenyl-1,3-dioxane.

1.4 Synthesis of 5-(2-methoxyethoxy)-2-phenyl-1,3-dioxane

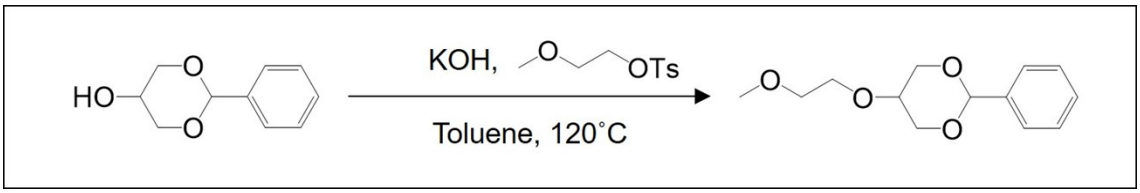

5-(2-methoxyethoxy)-2-phenyl-1,3-dioxane was synthesized in the same procedure as 5-(2-(2-(2-methoxyethoxy)ethoxy)ethoxy)-2-phenyl-1,3-dioxane, except that 2-methoxyethyl 4-methylbenzenesulfonate (13.8 g, 60 mmol) was used instead of 2-(2-methoxyethoxy)ethyl 4-methylbenzenesulfonate (19 g, 60 mmol). The reaction mixture was extracted by H_2O and CH_2Cl_2 to collect the organic layer. Then, the crude was purified by silica gel chromatography using hexane/ethyl acetate (1/1, v/v) to obtain (3 g, 12.6 mmol, yield 22%).

^{1}H NMR ($CDCl_3$, 400 MHz) δ:7.50 (m, 2H), 7.38—7.30 (m, 3H), 5.55 (s, 1H), 4.36 (d, 2H), 4.05 (d, 2H), 3.79—3.52 (m, 5H), 3.38 (s, 3H).
FT-IR(cm^{-1}): 2856, 1452,1390, 1091.
HRMS (CI) calcd for $C_{13}H_{19}O_4$ 327.1808 [M + H] found 327.1802.

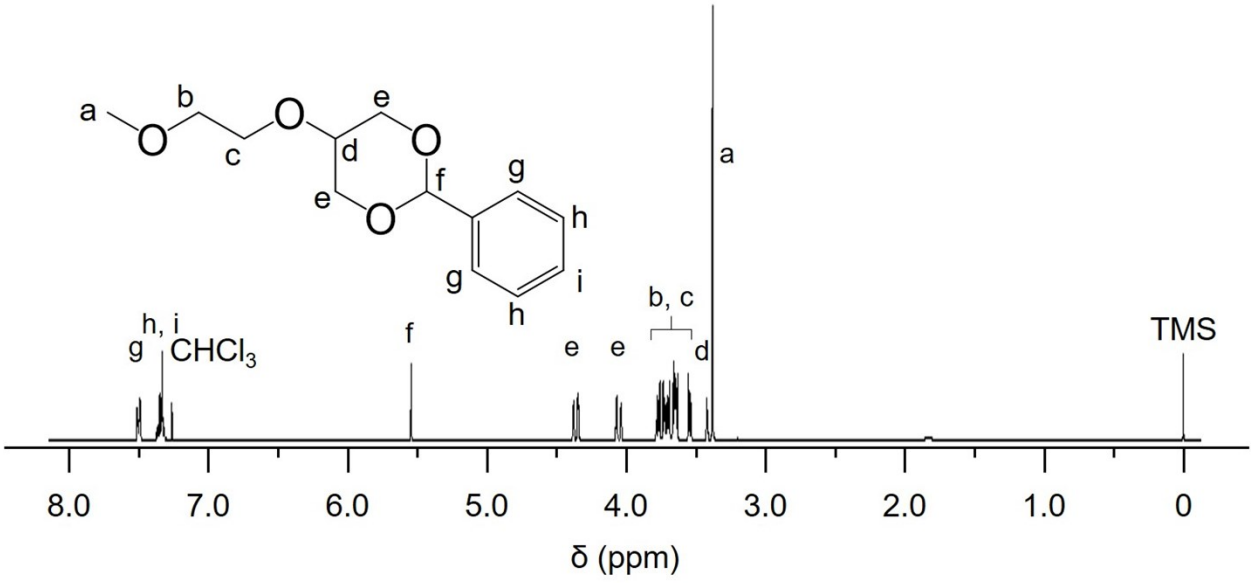

Figure S3. ^{1}H NMR spectrum for 5-(2-methoxyethoxy)-2-phenyl-1,3-dioxane.

1.5 Synthesis of 2-(2-(2-(2-methoxyethoxy)ethoxy)ethoxy)propane-1,3-diol(diol-*g*-OEG$_3$)

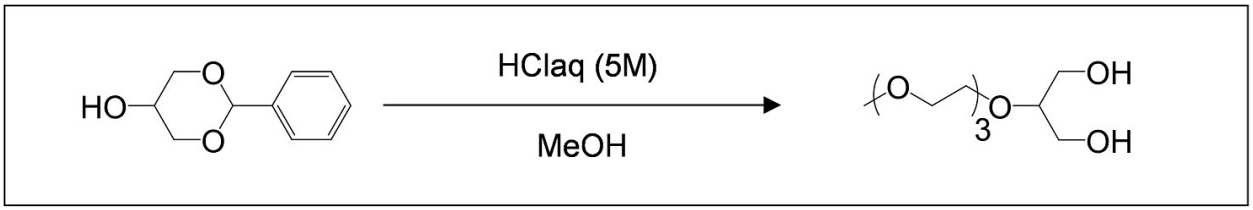

The deprotection of the acetal of benzaldehyde on 5-(2-(2-(2-methoxyethoxy)ethoxy)ethoxy)-2-phenyl-1,3-dioxane (9.1 g, 28 mmol) was achieved by stirring with 5 M HClaq in 100 mL of MeOH. The reaction mixture was extracted by H_2O and CH_2Cl_2 to collect the water layer. A total 5.7 g of diol-*g*-OEG$_3$ was obtained (5.7 g, 24 mmol, yield 86%).

^{1}H NMR ($CDCl_3$, 400 MHz) δ: 3.85—3.52 (m, 17H), 3.38 (s, 3H), 2.83 (t, 2H).
FT-IR(cm^{-1}): 3415, 2874, 1452, 1093.
HRMS (CI) calcd for $C_{10}H_{23}O_6$ 239.1495 [M + H] found 239.1487.

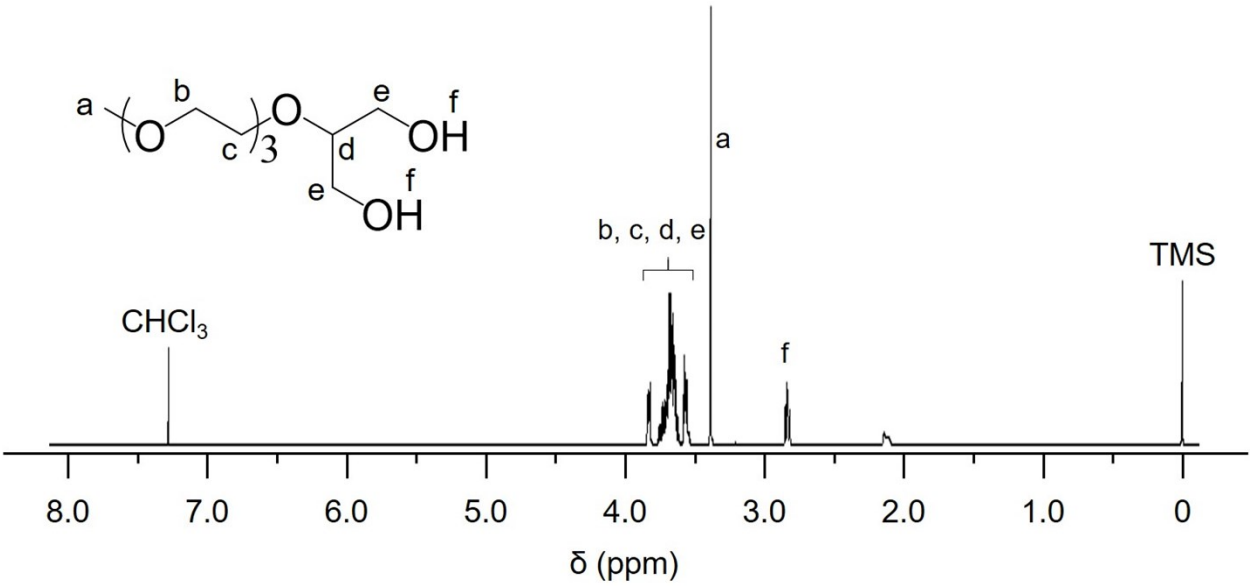

Figure S4. ^{1}H NMR spectrum for diol-*g*-OEG$_3$.

1.6 Synthesis of 2-(2-(2-methoxyethoxy)ethoxy)propane-1,3-diol(diol-*g*-OEG_2)

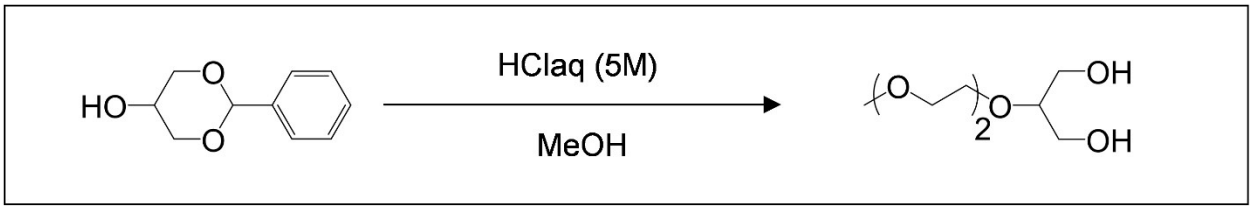

Diol-*g*-OEG_2 was synthesized in the same procedure as diol-*g*-OEG_3, except that 5-(2-(2-methoxyethoxy)ethoxy)-2-phenyl-1,3-dioxane (5.6 g, 20 mmol) was used instead of 5-(2-(2-(2-methoxyethoxy)ethoxy)ethoxy)-2-phenyl-1,3-dioxane (19.1 g, 28 mmol). The reaction mixture was extracted by H_2O and CH_2Cl_2 to collect the water layer. A total 5.7 g of diol-*g*-OEG_3 was obtaind (3.5 g, 18 mmol, yield 90%).

^{1}H NMR ($CDCl_3$, 400 MHz) δ: 3.85—3.52 (m, 12H), 3.38 (s, 3H), 2.83 (s, 2H).
FT-IR(cm^{-1}): 3404, 2872, 1454, 1076.
HRMS (ESI) calcd for $C_8H_{18}Na_1O_5$ 217.10519 [M + Na] found 217.10599.

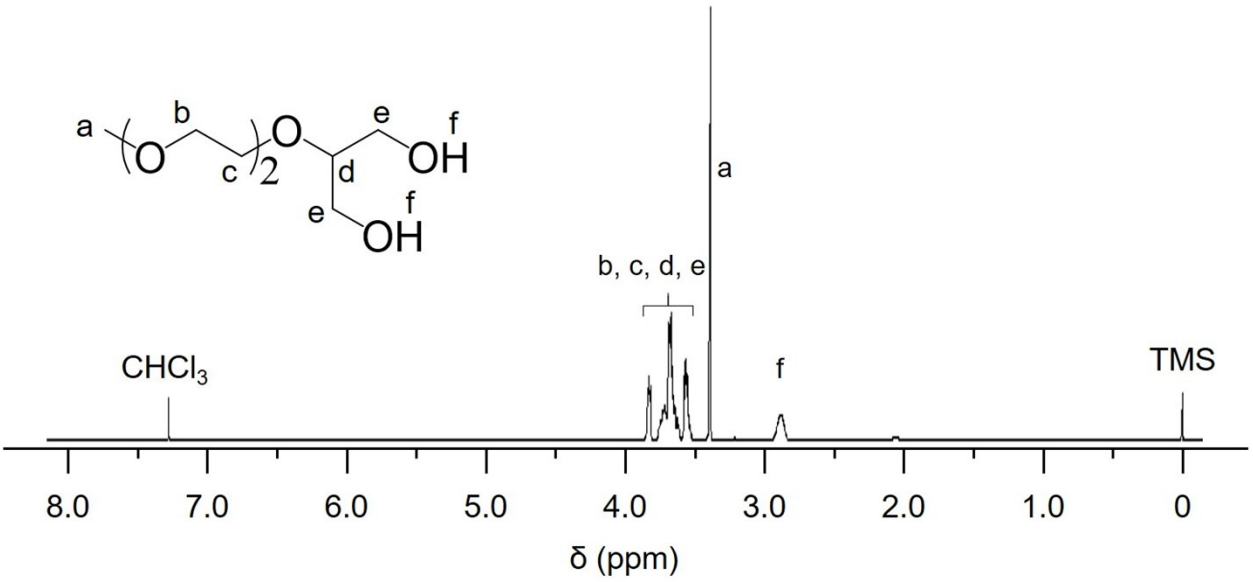

Figure S5. ^{1}H NMR spectrum for diol-*g*-OEG_2.

1.7 Synthesis of 2-(2-methoxyethoxy)propane-1,3-diol(diol-*g*-OEG$_1$)

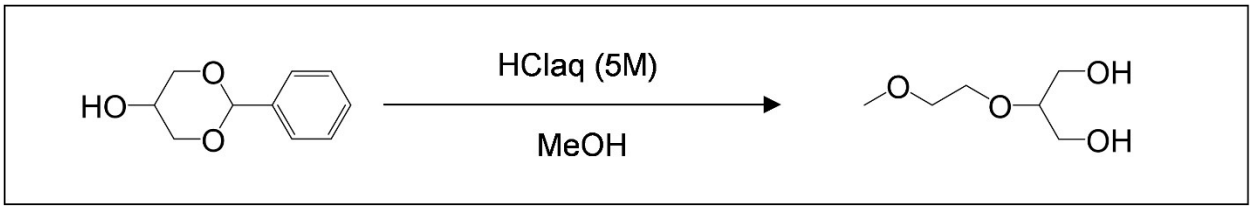

Diol-*g*-OEG$_1$ was synthesized in the same procedure as diol-*g*-OEG$_3$, except that 5-(2-methoxyethoxy)-2-phenyl-1,3-dioxane (2.4 g, 10 mmol) was used instead of 5-(2-(2-(2-methoxyethoxy)ethoxy)ethoxy)-2-phenyl-1,3-dioxane (19.1 g, 28 mmol). The reaction mixture was extracted by H_2O and CH_2Cl_2 to collect the water layer. A total 5.7 g of diol-*g*-OEG$_3$ was obtained (1.4 g, 9 mmol, yield 90%).

^{1}H NMR ($CDCl_3$, 400 MHz) δ: 3.88—3.30 (m, 9H), 3.38 (s, 3H), 2.83 (s, 2H).
FT-IR(cm^{-1}): 3377, 2875, 1456, 1074.
HRMS (ESI) calcd for $C_6H_{14}Na_1O_4$ 173.07898 [M + Na] found 173.07909.

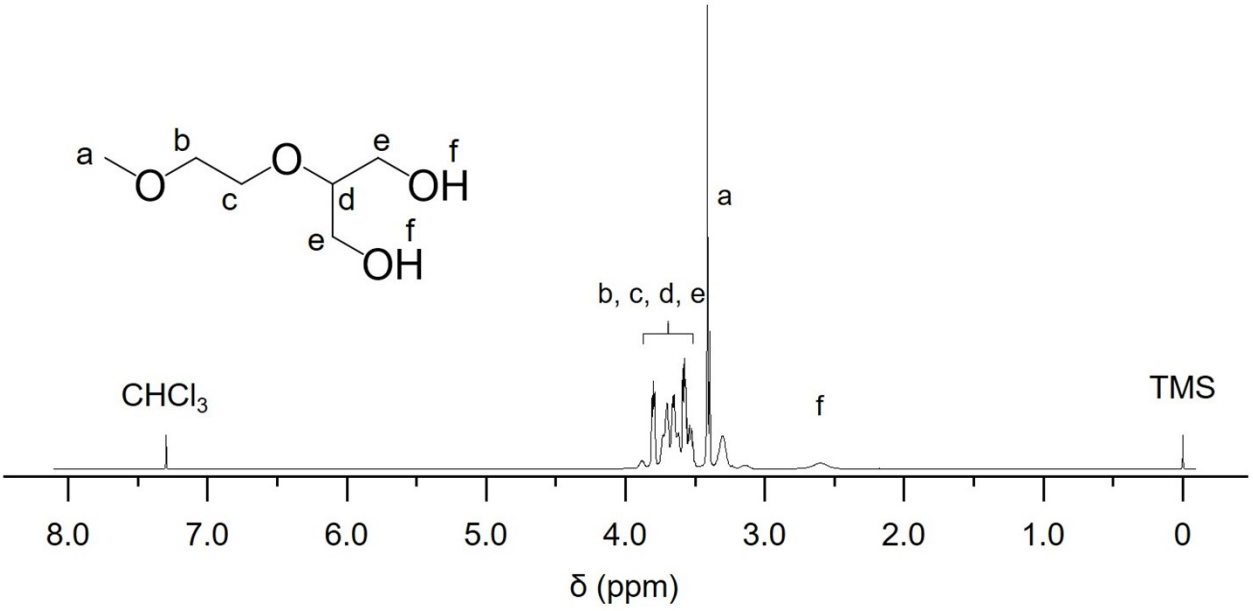

Figure S6. ^{1}H NMR spectrum for diol-*g*-OEG$_1$.

1.8 Polymerization

The typical procedure for polymerization was as follows. Diol monomers (4 mmol) was added to 20 mL vial with septum rubber and dried under vacuum at 60˚C overnight. After the atmosphere in the vial was changed to N_2 condition, one dropwise of DBTDL, 4 mL of anhydrous THF, HMDI (4 mmol) was add to the vial under N_2 condition and stirred at 60˚C for 4 h. After the reaction, resultant polymer was precipitated into excess amount of diethyl ether.

2. SEC profile

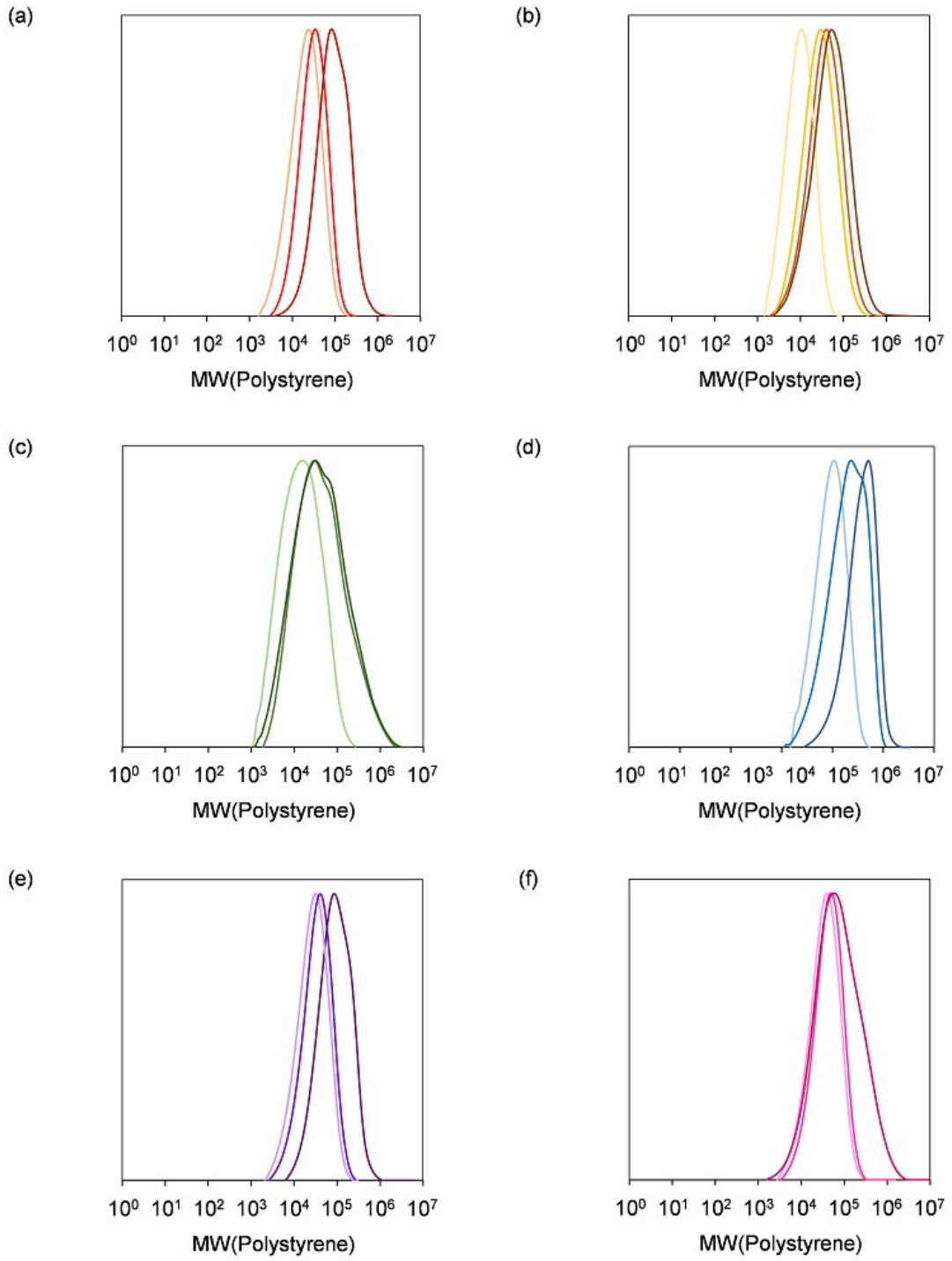

Figure S7. SEC profiles for PU-*g*-OEG_3(a), PU-*g*-OEG_2(b), PU-*g*-OEG_1(c), PU-*l*-OEG_5(d), PU-*l*-OEG_4(e), PU-*l*-OEG_3(f).

3. FT-IR spectra

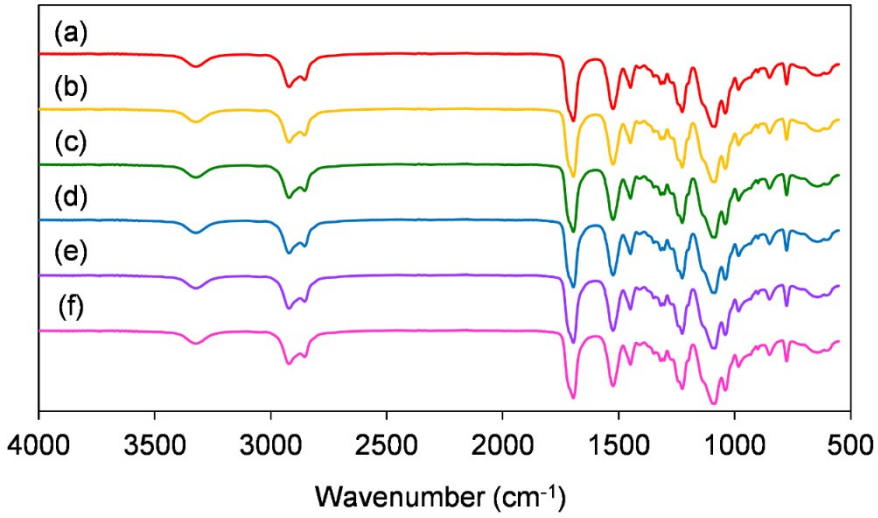

Figure S8. FT-IR spectra for PU-*g*-OEG_3(a), PU-*g*-OEG_2(b), PU-*g*-OEG_1(c), PU-*l*-OEG_5(d), PU-*l*-OEG_4(e), PU-*l*-OEG_3(f).

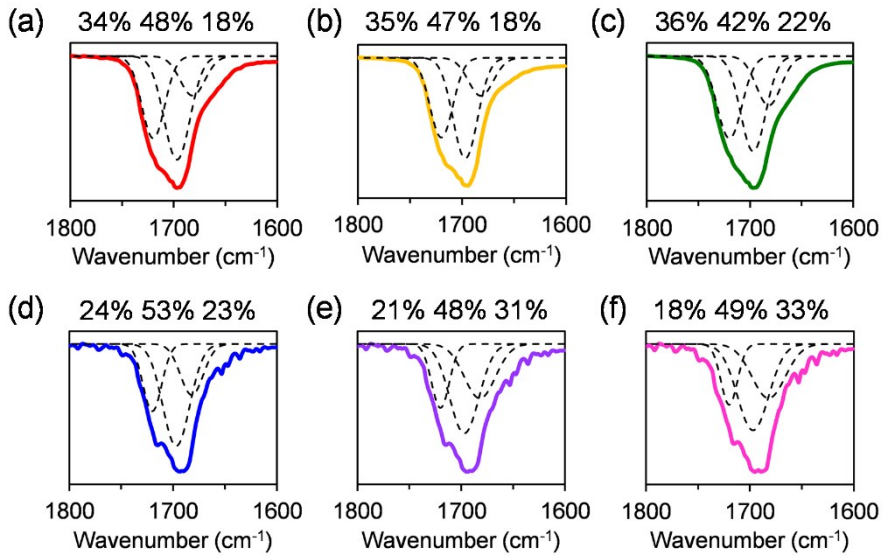

Figure S9. C=O vibration peak fitting on FT-IR spectra for PU-*g*-OEG_3(a), PU-*g*-OEG_2(b), PU-*g*-OEG_1(c), PU-*l*-OEG_5(d), PU-*l*-OEG_4(e), PU-*l*-OEG_3(f).

4. Tensile test

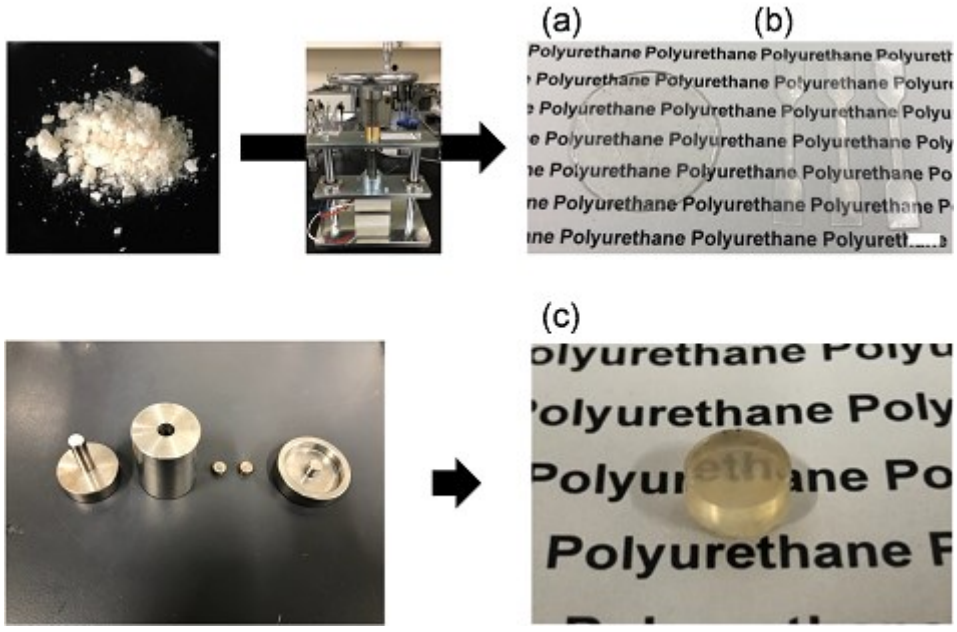

Figure S10. Photograph for Hotpress film(a), tensile test piece(b), cylinder PU(c).

Table S1. Summary of mechanical properties.

Sample	Stress at break σ_b (MPa)	Strain at break ε_b (%)	Young modulus E (MPa)	Toughness U_t (MJ/m3)	Yielding σ_y (MPa)
PU-*g*-OEG_3-119k	49.0 ± 3.5	219.3 ± 17.0	524.2 ± 28.1	74.5 ± 8.4	36.5 ± 1.0
PU-*g*-OEG_3-38k	34.4 ± 2.4	187.3 ± 4.8	435.2 ± 31.1	52.0 ± 1.5	31.2 ± 2.1
PU-*g*-OEG_3-25k	31.9 ± 1.1	186.9 ± 16.1	317.1 ± 25.6	40.5 ± 7.9	23.2 ± 2.1
PU-*g*-OEG_2-72k	34.3 ± 1.9	124.2 ± 21.4	481.2 ± 25.7	37.4 ± 6.2	37.3 ± 2.2
PU-*g*-OEG_2-49k	24.9 ± 1.2	168.5 ± 14.9	350.1 ± 7.4	33.5 ± 3.0	24.4 ± 0.3
PU-*g*-OEG_2-12k	3.3 ± 0.1	4.0 ± 1.5	207.9 ± 75.2	0.1 ± 0.0	
PU-*g*-OEG_1	63.0 ± 3.6	19.0 ± 4.0	563.1 ± 6.0	7.9 ± 2.4	
PU-*l*-OEG_5	21.3 ± 2.5	300.9 ± 23.4	389.0 ± 21.3	54.4 ± 2.5	25.4 ± 0.4
PU-*l*-OEG_4	14.4 ± 2.4	255.5 ± 39.8	198.9 ± 53.5	32.2 ± 9.5	14.2 ± 2.8
PU-*l*-OEG_3	38.6 ± 0.9	311.9 ± 11.2	407.4 ± 65.1	106.7 ± 6.8	49.8 ± 0.7
PU-*l*-PDO	38.2 ± 6.3	4.8 ± 1.0	902.0 ± 122.2	1.2 ± 0.4	

5. Rheology

Table S2. Summary of rheological properties.

Sample	M_n (kg/mol)	M_w/M_n	C1	C2	η_0 (Pa s)	G_N^0 (MPa)	n_{sc}	n_g
PU-*g*-OEG$_3$	13.2	1.91	9	110	2.1×10^7	0.77	5.5	9
PU-*g*-OEG$_3$	22.7	1.66	8	100	6.3×10^7	0.88	5.5	9
PU-*g*-OEG$_3$	58.1	2.04	9	120	1.4×10^9	0.98	5.5	9
PU-*g*-OEG$_2$	7.1	1.63	9	120	2.7×10^6	0.76	4	9
PU-*g*-OEG$_2$	22.8	2.16	8	120	4.2×10^7	0.98	4	9
PU-*g*-OEG$_2$	28.6	2.51	10	100	1.7×10^8	0.99	4	9
PU-*g*-OEG$_1$	18.2	4.71	9	120	1.2×10^8	0.95	2.5	9
PU-*l*-OEG$_5$	6.9	1.54	7	120	1.1×10^4	1.0	—	—
PU-*l*-OEG$_5$	12.3	1.97	9	90	1.0×10^7	1.4	—	—
PU-*l*-OEG$_5$	26.8	1.57	9	90	2.6×10^7	1.6	—	—
PU-*l*-OEG$_4$	17.7	1.88	8	90	8.3×10^6	1.2	—	—
PU-*l*-OEG$_4$	57.7	2.00	8	100	5.2×10^7	1.4	—	—
PU-*l*-OEG$_3$	23.1	1.84	8	100	2.1×10^6	0.95	—	—
PU-*l*-PDO								

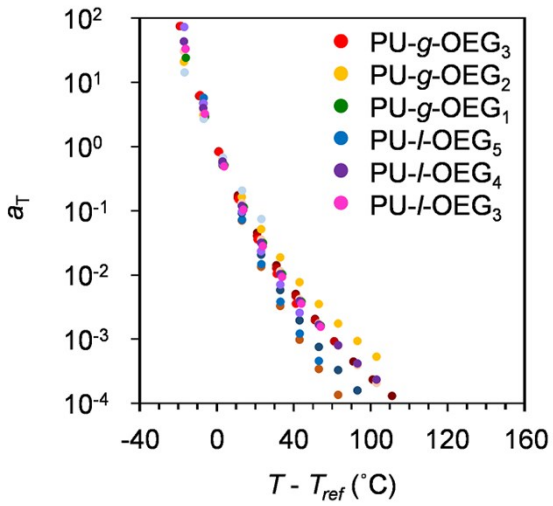

Figure S11. Shift factors for PU derivatives ($T_{ref} = T_g + 50$ ˚C).

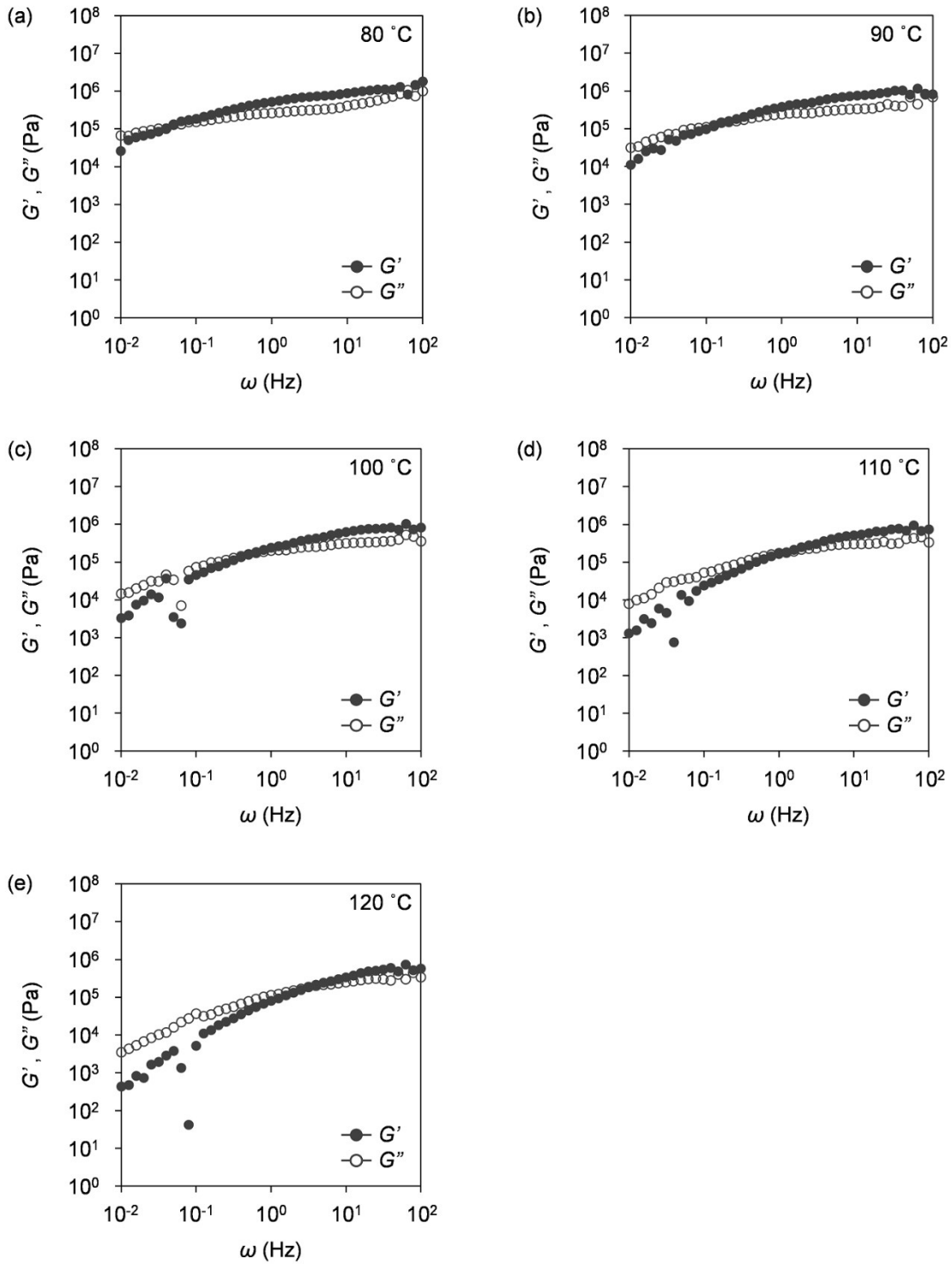

Figure S12. *G′* and *G″* curves for PU-*g*-OEG$_3$ with 80 ˚C (a), 90 ˚C (b), 100 ˚C (c), 110 ˚C (d), and 120 ˚C (e).

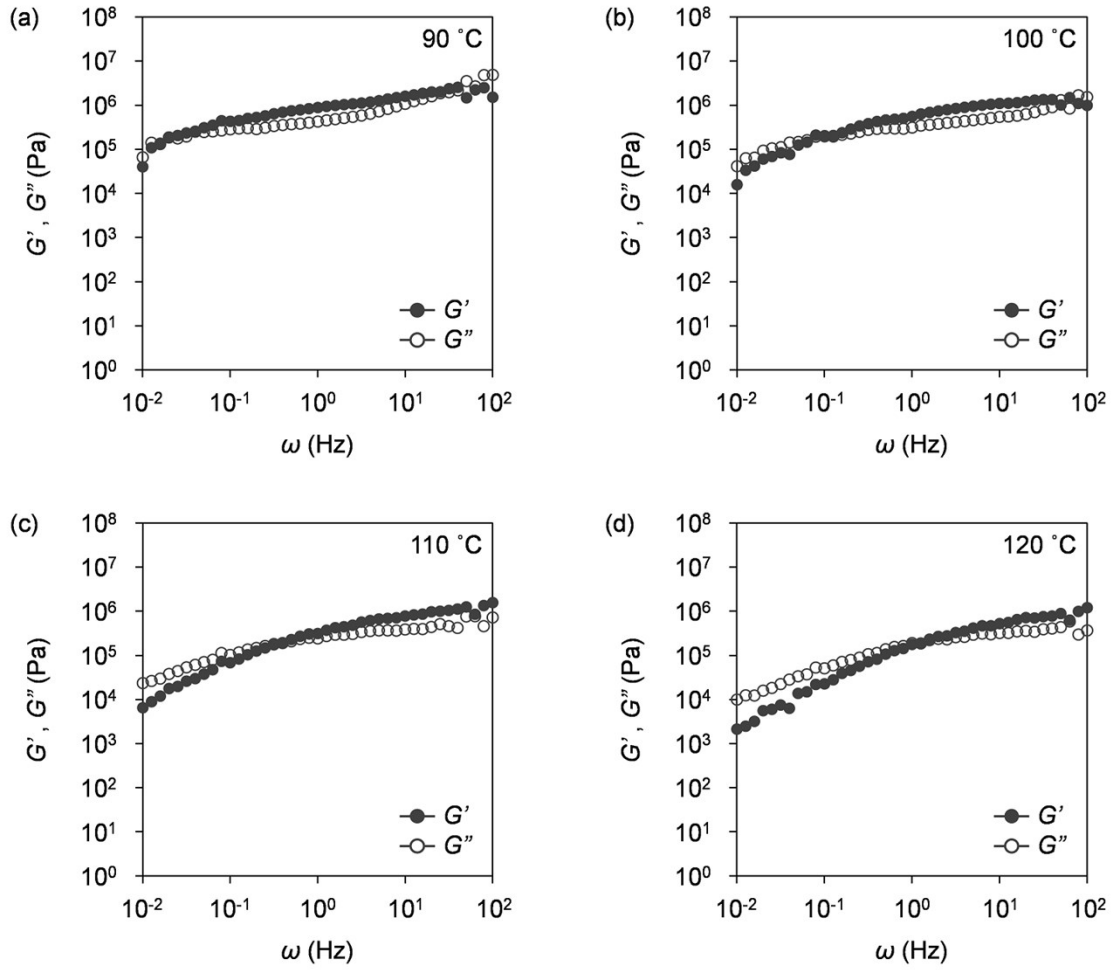

Figure S13. *G′* and *G″* curves for PU-*g*-OEG_2 with 90 ˚C (a), 100 ˚C (b), 110 ˚C (c), and 120 ˚C (d).

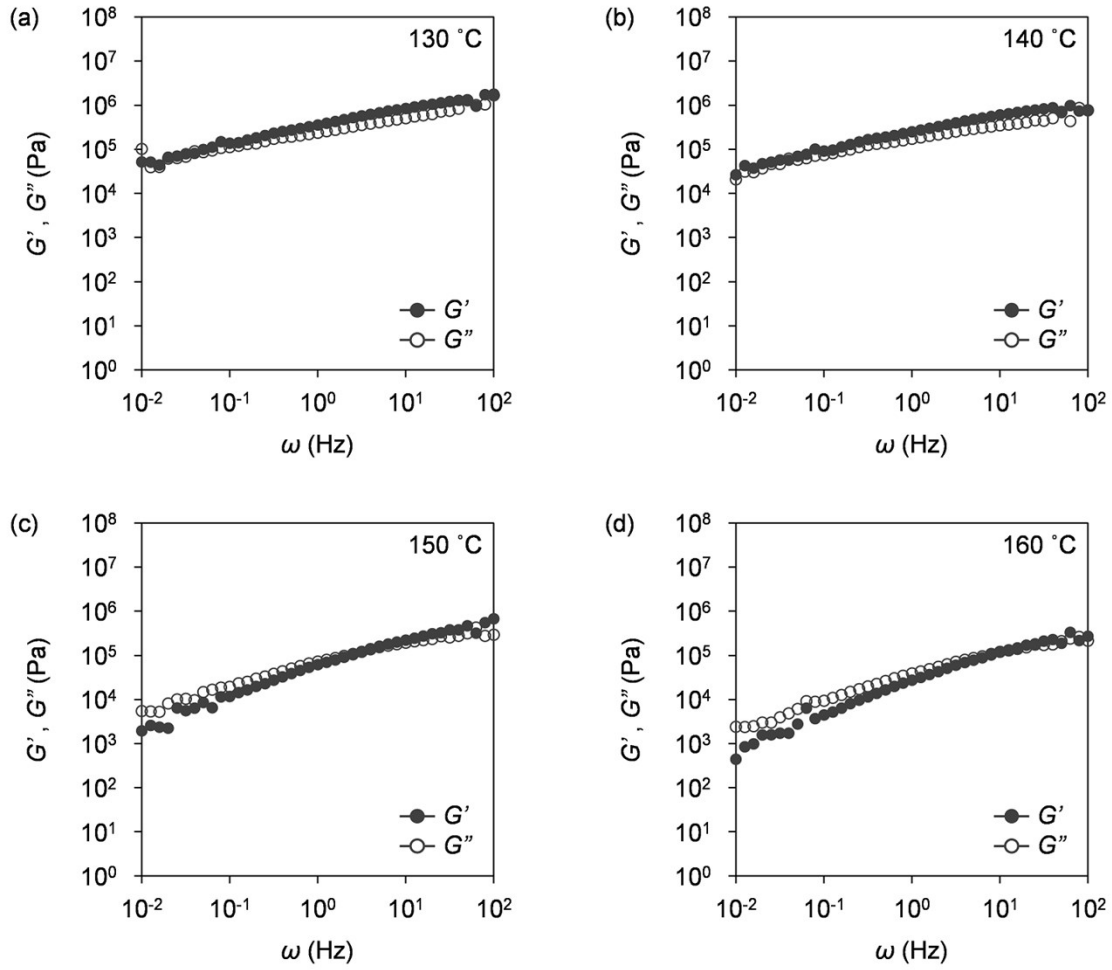

Figure S14. *G′* and *G″* curves for PU-*g*-OEG$_1$ with 130 ˚C (a), 140 ˚C (b), 150 ˚C (c), and 160 ˚C (d).

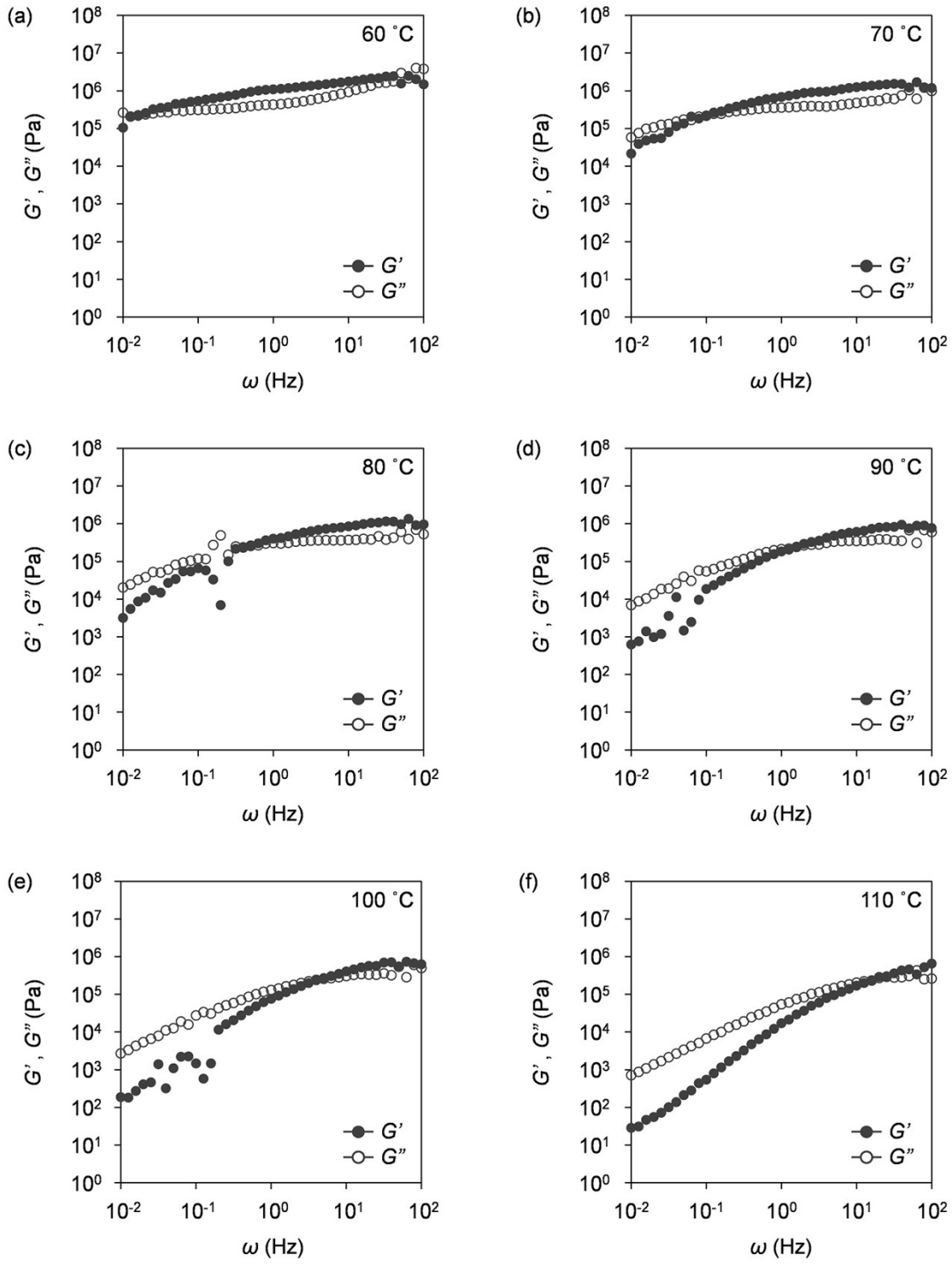

Figure S15. *G′* and *G″* curves for PU-*l*-OEG_5 with 60 ˚C (a), 70 ˚C (b), 80 ˚C (c), 90 ˚C (d), 100 ˚C (e), and 110 ˚C (f).

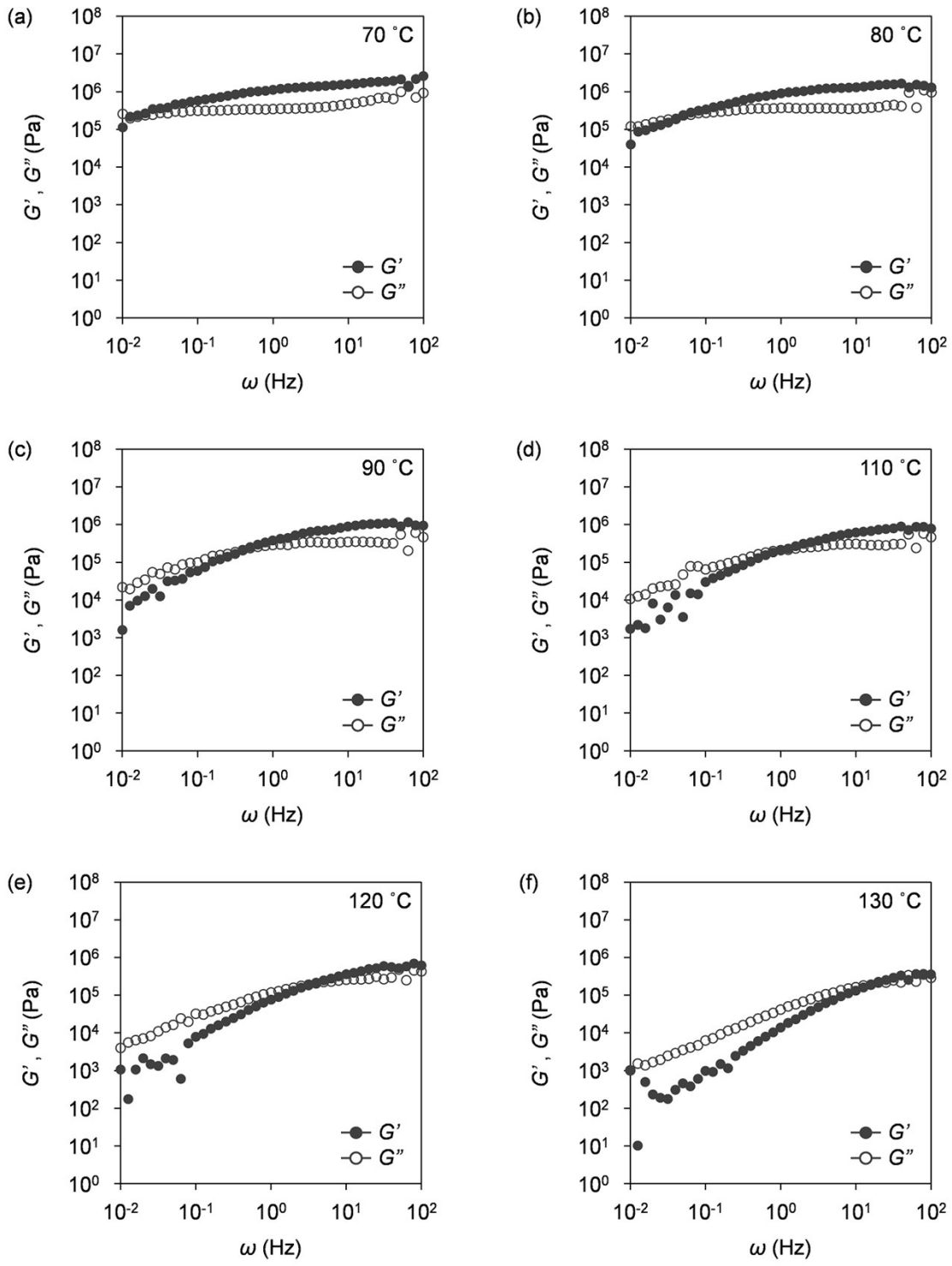

Figure S16. *G′* and *G″* curves for PU-*l*-OEG$_4$ with 70 ˚C (a), 80 ˚C (b), 90 ˚C (c), 110 ˚C (d), 120 ˚C (e), and 130 ˚C (f).

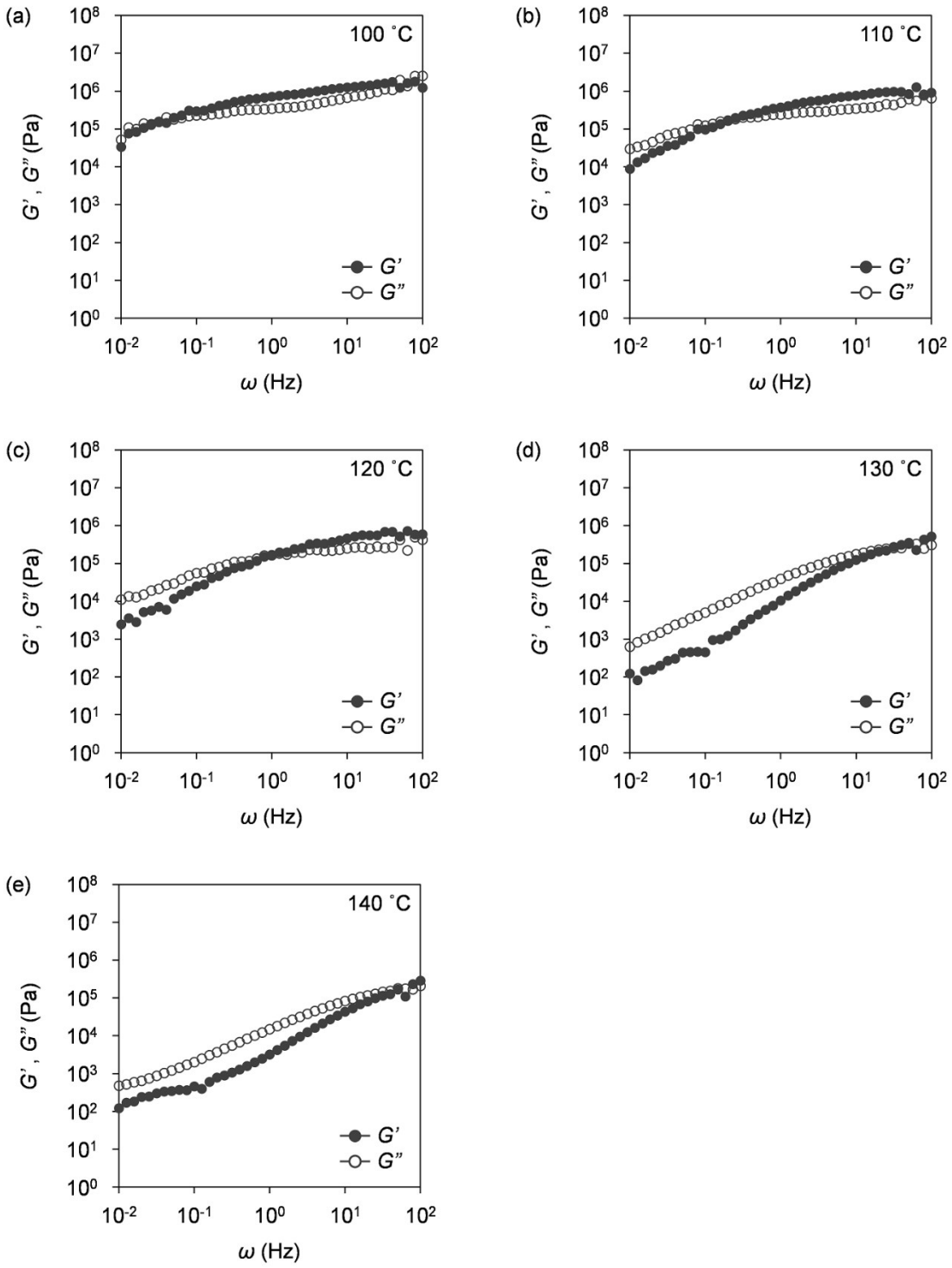

Figure S17. *G′* and *G″* curves for PU-*l*-OEG$_3$ with 100 ˚C (a), 110 ˚C (b), 120 ˚C (c), 130 ˚C (d), and 140 ˚C (e).

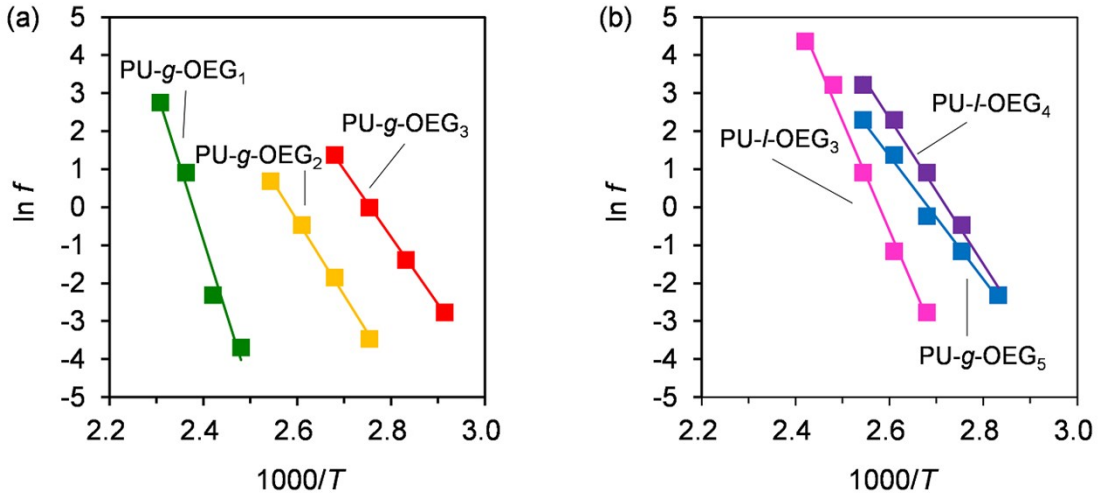

Figure S18. Arrhenius plots for PU-*g*-OEG_3(a), PU-*g*-OEG_2(b), PU-*g*-OEG_1(c), PU-*l*-OEG_5(d), PU-*l*-OEG_4(e), PU-*l*-OEG_3(f).

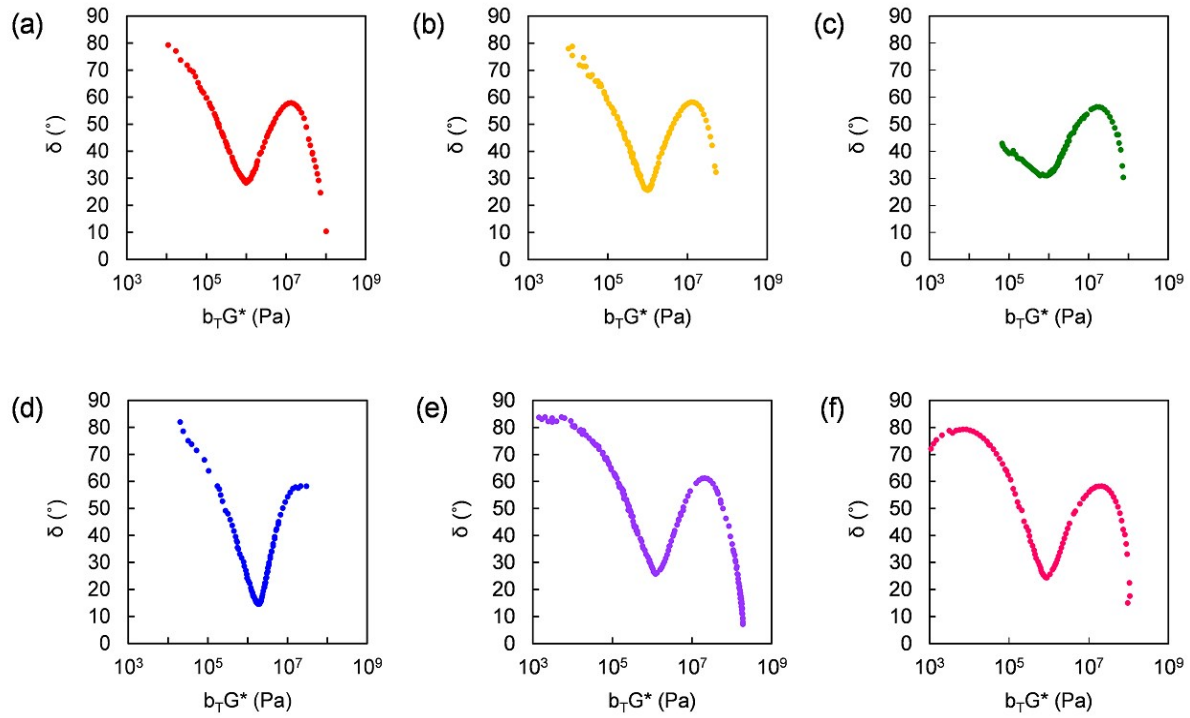

Figure S19. Van Gurp-Palmen curves for PU-*g*-OEG_3(a), PU-*g*-OEG_2(b), PU-*g*-OEG_1(c), PU-*l*-OEG_5(d), PU-*l*-OEG_4(e), PU-*l*-OEG_3(f).

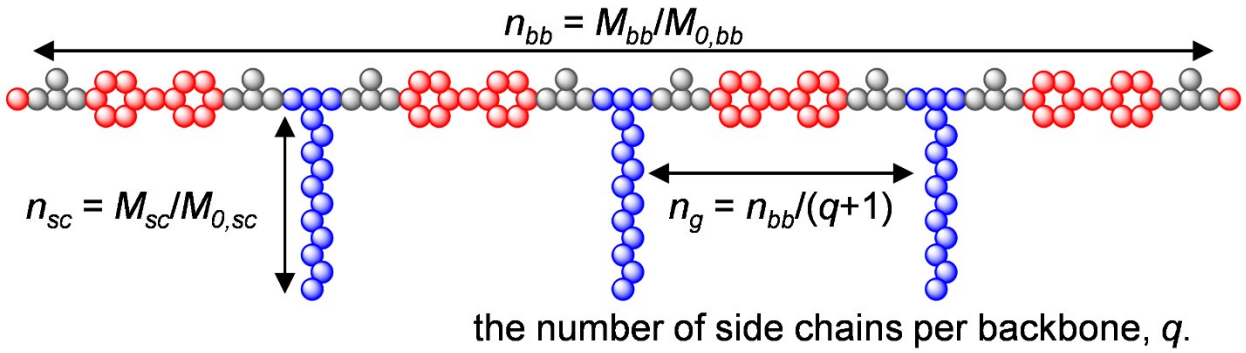

Figure S20. Structural parameter for comb PUs.

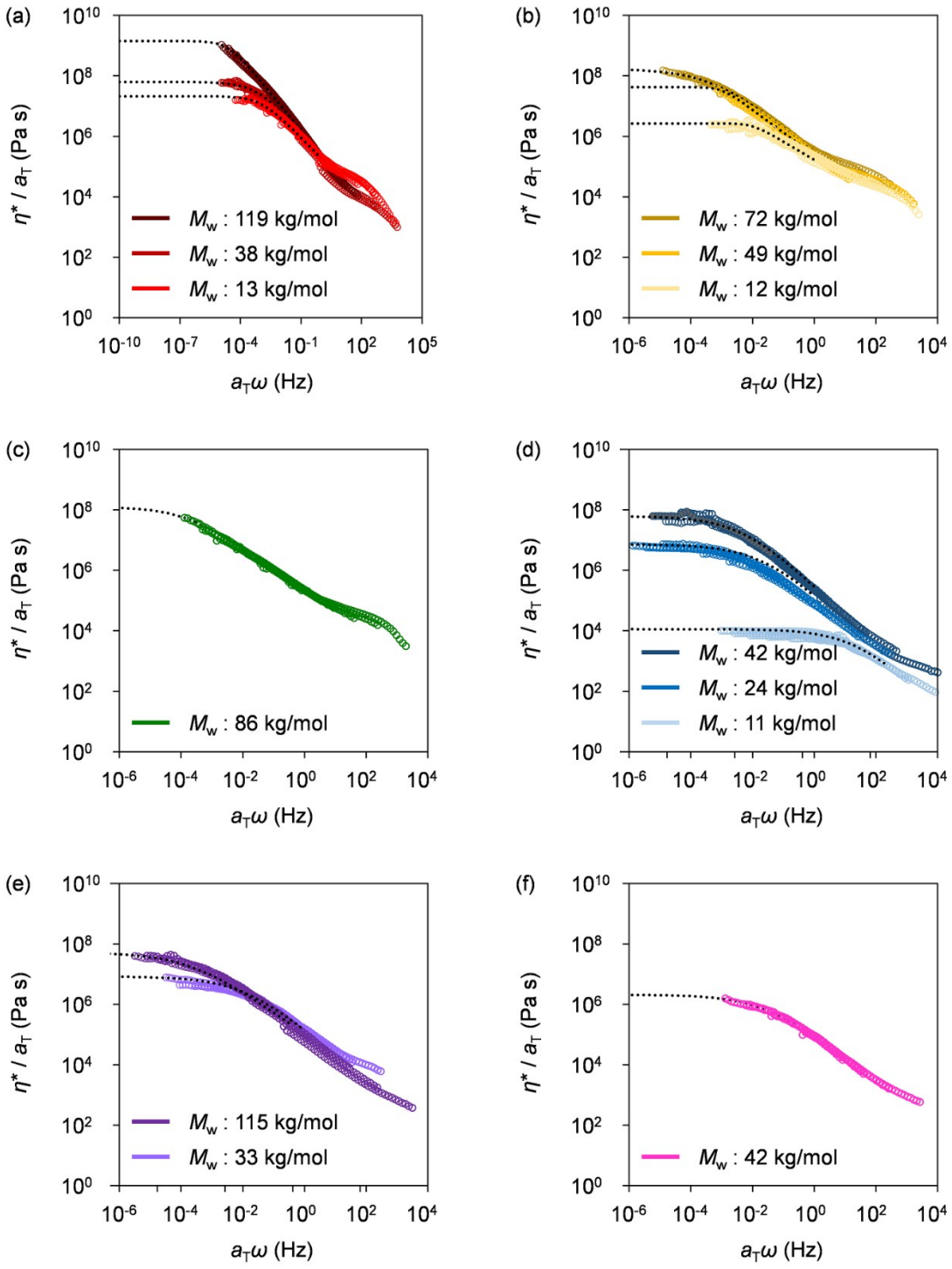

Figure S21. Reduced complex viscosity versus reduced frequency for PU-*g*-OEG_3 (a), PU-*g*-OEG_2 (b), PU-*g*-OEG_1 (c), PU-*l*-OEG_5 (d), PU-*l*-OEG_4 (e), and PU-*l*-OEG_3 (f). Dashed fitting curves were calculated by Carreau-Yasuda model equation.[2]

6. Reference

Zheng, Z., Luo, M., Yu, J., Wang, J., & Ji, J. (2012). Novel process for 1, 3-dihydroxyacetone production from glycerol. 1. Technological feasibility study and process design. *Industrial & engineering chemistry research*, *51*(9), 3715-3721.

Yasuda, K. Y., Armstrong, R. C., & Cohen, R. E. (1981). Shear flow properties of concentrated solutions of linear and star branched polystyrenes. *Rheologica Acta*, *20*(2), 163-178.